Journal of Environmental Management 324 (2022) 116247

Contents lists available at ScienceDirect

Journal of Environmental Management

journal homepage: www.elsevier.com/locate/jenvman

Research article

Recovery of structural extracellular polymeric substances (sEPS) from aerobic granular sludge: Insights on biopolymers characterization and hydrogel properties for potential applications

Riccardo Campo [a,*], Emiliano Carretti [b], Claudio Lubello [a], Tommaso Lotti [a]

[a] Department of Civil and Environmental Engineering – (DICEA), University of Florence, Florence, Italy
[b] Department of Chemistry "Ugo Schiff" & CSGI Consortium, University of Florence, Italy

ARTICLE INFO

Keywords:
sEPS
Aerobic granular sludge
Hydrogel rheological properties
Resource recovery
Water holding capacity
WRRFs

ABSTRACT

Nowadays, wastewater treatment plants (WWTPs) are transforming into water resource recovery facilities (WRRFs) where the resource recovery from waste streams is pivotal. Aerobic granular sludge (AGS) is a novel technology applied for wastewater treatment. Extracellular polymeric substances (EPS) secreted by microorganisms promote the aggregation of bacterial cells into AGS and the structural fraction of EPS (sEPS) is responsible for the mechanical properties of AGS. sEPS can be extracted and recovered from waste AGS by physico-chemical methods and its characterization is to date of relevant concern to understand the properties in the perspective of potential applications. This study reports on: characterization of sEPS extracted and recovered from AGS; - formation and characterization of sEPS-based hydrogels. Briefly, sEPS were extracted by a thermo-alkaline process followed by an acidic precipitation. sEPS-based hydrogels were formed by a cross-linking process with a 2.5% w/w $CaCl_2$ solution. The following key-findings can be drawn: i) hydrogels can be formed starting from 1% w/w sEPS on, by diffusion of Ca^{2+} into sEPS network; ii) the Ca/C molar ratio of hydrogels decreased with increasing concentration of sEPS from 1 to 10% w/w; iii) the thermogravimetric and spectroscopic behaviours of sEPS show that the cross-linking reaction mainly involves the polysaccharidic fraction of biopolymers; iv) water-holding capacity up to 99 gH_2O/g_{sEPS} was registered for 1% w/w sEPS-based hydrogels, suggesting applications in several industrial sectors (i.e. chemical, paper, textile, agronomic, etc.); v) rheological results highlighted a solid-like behaviour (G'≫G") of sEPS-based hydrogels. The power-law fitting of G' vs. sEPS concentration suggests that the expansion of the sEPS network during cross-linking occurs through a percolative mechanism involving the initial formation of sEPS oligomers clusters followed by their interconnection towards the formation of 3D network. These findings provide additional information about the mechanisms of sEPS-based hydrogel formation and reveal the peculiar physico-chemical characteristics of sEPS which nowadays are increasingly gaining interest in the context of resource recovery.

1. Introduction

Over the last two decades, aerobic granular sludge (AGS) occupies a relevant position among the most promising technologies for wastewater treatment (Campo et al., 2020b; Pronk et al., 2015). To date, more than 80 full-scale AGS wastewater treatment plants (WWTPs) are present all over the world (DHV-Nereda®Plants, 2021). Granules are pseudo-spherical biofilms made of self-aggregated microorganisms, having high density, high settling velocity (up to 100 m/h) and a multi-layered structure with different redox potential conditions due to e-donors and e-acceptors radial concentration gradients (Pronk et al., 2020). This makes AGS technology suitable for simultaneous removal of carbon, nitrogen and phosphorus due to the presence of aerobic, anoxic and anaerobic micro-environments and the growing of a diversified bacterial consortium mainly composed by phosphorus accumulating organisms (PAOs and denitrifying PAOs), glycogen accumulating organisms (GAOs and denitrifying GAOs), ammonia oxidizing bacteria (AOBs), nitrite oxidizing bacteria (NOBs), ordinary heterothrophic organisms (OHOs).

As in all kinds of biofilms, bacterial cells in aerobic granules are embedded in extracellular polymeric substances (EPS).

EPS are a complex mixture of biopolymers that provide mechanical

* Corresponding author.
E-mail address: riccardo.campo@unifi.it (R. Campo).

https://doi.org/10.1016/j.jenvman.2022.116247
Received 21 June 2022; Received in revised form 7 September 2022; Accepted 9 September 2022
Available online 26 September 2022

and structural stability thut allowing biofilm cells to establish microconsortia, enhance water holding and nutrient sorption, provide protection against viruses, antimicrobials and disinfectants, and act a keyrole in nutrient recycling (Flemming and Wingender, 2010). These properties can be provided by a several biopolymers such as polysaccharides, proteins and nucleic acids. EPS are produced by different specific microorganisms and may have different characteristics as a function of time or environmental conditions (Seviour et al., 2019).

In AGS biofilms, a fraction of EPS is considered responsible for the mechanical properties of aerobic granular sludge and can be extracted from pristine granules by physico-chemical methods: the so called structural EPS (sEPS) (Lin et al., 2010; Seviour et al., 2012). sEPS form a highly hydrated matrix presenting gelling properties that confers stiffness to the morphology of AGS and provide mechanical strength for granules, thus ensuring biomass retention and the stable operation of the AGS reactor (Li et al., 2020). sEPS are constituted by several compounds (i.e. polysaccharides, proteins, exoenzymes, lipids, nucleic acids, humic acids, fulvic acids etc.) (Felz, 2019; Flemming and Wingender, 2010; Lin et al., 2010; Pronk et al., 2020) but, at the time of writing, their composition is not fully known. Recent studies revealed that AGS bacteria produce exopolymers as glycoproteins, sulphated glycosaminoglycan-like, hyaluronic acid-like, and sialic acids containing compounds (de Graaff et al., 2019; Felz et al., 2020b; Lin et al., 2018).

Recently, the possibility to extract the sEPS from AGS, has opened new scenarios on biopolymers recovery from AGS (Amorim de Carvalho et al., 2021; Felz et al., 2016; Kehrein et al., 2020; Seviour et al., 2019) as well as the reduction of waste sludge disposal. Several methods have been tested for sEPS extraction from AGS and thermo-alkaline conditions with Na_2CO_3 resulted in the highest yield factor compared to other techniques (Felz et al., 2016). Regarding the potential applications of sEPS, recent studies revealed promising effects as flame retardants, both as pure coating (Kim et al., 2020) or as composite coating with Polyvinyl alcohol (PVA) (Kim et al., 2022). This effect was mainly due to the phosphates contained in sEPS that enhanced char formation and inhibited the pyrolysis of textile fibers. sEPS could stimulate the root growth of plants due to the water holding capacity of sEPS and the possibility to promote a slow nutrients release in soils (ROYAL HASKONINGDHV, 2020). sEPS could also be applied as surface coating material. Due to their amphiphilic property, sEPS can form a film on a hydrophilic surface like paper/textile thus acting as a water-resistant barrier (Lin et al., 2015). In wastewater bioremediation, sEPS were recently applied as bio-flocculants due to their property to increase the cell adhesion (Amin Vieira da Costa et al., 2022) and heavy metals adsorbers (i.e. Pb^{2+}, Cd^{2+}, Zn^{2+}, etc.) due to the ability to bind divalent cations onto their functional groups (Felz et al., 2020a; Liu et al., 2015). In the building industry, sEPS could be applied to improve the curing of cement. sEPS enhance the retention of cement surface humidity thus reducing moisture loss and preventing drying shrinkage and structural cracking (Karakas et al., 2020).

Hydrogel can be formed from sEPS through cross-linking process with divalent metal ions such as Ca^{2+} (Lin et al., 2008; Seviour et al., 2010). It was found that the stiffness of hydrogel strictly depends on the metal ion used as cross-linker (Felz et al., 2020a) and this can bring important implications in hydrogel applications and granule stability. To date there is a knowledge gap in literature regarding the mechanism of hydrogel formation from sEPS. More knowledge in this regard could shed light on the understanding if distinct gelling mechanisms, such as for alginate described egg-box model (Braccini and Pérez, 2001; Cao et al., 2020; Sikorski et al., 2007), are involved in the sEPS hydrogel formation.

The aim of this study is contributing to the increase of knowledge of the sEPS and sEPS-based hydrogels properties. The novelty of this research relies on a deep focus on sEPS and sEPS-based hydrogels with the purpose of improve the knowledge in this field in line with resource recovery. Particular attention is paid to the mechanisms of hydrogels formation upon cross-linking by diffusion with calcium for a wide range of concentration of aqueous sEPS solutions (from 1% w/w up to about 10% w/w). Hydrogels were characterized in terms of elemental composition, thermogravimetric behaviour, water-holding capacity, and rheological properties. The interest and novelty in studying the hydrogel formation mechanism and the relation with sEPS concentration is twofold: understanding the relationship between the sEPS hydrogel formation and AGS stability in WWTP; - understanding hydrogels' properties in view of potential applications in the field of resource recovery.

2. Materials and methods

2.1. Structural extracellular polymeric substances extraction and hydrogel formation

sEPS were extracted from waste AGS according to previous report by Felz et al. (2016) (Felz et al., 2016). A 6% w/w (weight) of granules were put in a 250 mL baffled flask, mixed with 0.5% (w/v) of Na_2CO_3 and stirred for 35 min at 400 rpm and 80 °C in water bath. Then, the mixture was transferred into 50 mL centrifugation tubes, and centrifuged at 4.000×*g*, 4 °C for 20 min. The supernatant, representing the total EPS, was dialyzed for 24 h against Milli-Q ultrapure water in 3.5 kDa molecular weight cut off (MWCO) dialysis bag (SnakeSkin™ Dialysis Tubing, 3.5K MWCO, 35 mm, Thermo Scientific™).

The dialysis water was changed after 12 h to enhance the driving-force effect of the dialysis. One molar HCl was added to EPS, to a final pH of 2.2 ± 0.05 thus extracting sEPS, in the acidic form, from total EPS. Then the extract was centrifuged at 4.000×*g*, 4 °C for 20 min to obtain a gel-like pellet of acidic sEPS. In order to resuspend the acidic sEPS pellet, a solution of 0.5 M NaOH was added while mixing the gel slowly with a glass stick by hand until pH 8.5 is reached. At this point, a homogeneous solution of sEPS was obtained.

Hydrogel formation was performed by diffusion of Ca^{2+} from a 2.5% w/w $CaCl_2$ cross-linking solution into the sEPS matrix through a dialysis membrane (SnakeSkin™ Dialysis Tubing, 3.5K MWCO, 35 mm, Thermo Scientific™). Nine sEPS solutions at increasing biopolymer concentration (~1–10% w/w) were prepared and placed in a 4.2 mL cylinder (Height/Diameter = 0.16). This cylinder was sealed at the bottom and top by two square sheets of dialysis membrane with a side of about 5 cm. Each cylinder was then put into 200 mL of 2.5% w/w $CaCl_2$ solution for 24h at room temperature (Fig.S1). After 24h of cross-linking with $CaCl_2$, cylindrical hydrogels were recovered by opening the carrier (Fig. S1a) and by removing the dialysis membrane sheets.

2.2. Physicochemical and FT-IR analysis

Total solids (TS) and volatile solids (VS) of sEPS and hydrogel were determined according to the standard methods (APHA/AWWA/WEF, 2017). Elemental analysis was performed for sEPS and hydrogels according to the standard methods (APHA/AWWA/WEF, 2017) with a FLASH 1112 EA/Soil instrument (Thermo®).

The bicinchoninic acid (BCA) assay (Smith et al., 1985) was applied in this study for proteins (PN) determination, since it was proved that it shows less variability for different proteins than Lowry's method (Lowry et al., 1951). Analysis was performed using the commercial BCA assay protein quantification (Interchim). The standard curves were determined with BSA (bovine serum albumin) and cytochrome C, measuring the absorbance at 562 nm wavelength. Polysaccharides (PS) were determined with the anthrone sulfuric acid method (Dreywood, 1946), using d-glucose as standard.

Fourier transform InfraRed (FT-IR) spectra were collected in transmittance mode, by dispersing the sample powder in a KBr pellet, using a FTS-40, BioRad (USA), resolution of 4 cm^{-1} and 64 scans.

Table 1
sEPS characterization.

Parameter	Unit	This study	Reference studies	
VS/TS, AGS (105°C)	gVS_{AGS}/gTS_{AGS}	0.81 ± 0.01	0.87[a]	–
VS/TS, sEPS (105°C)	gVS_{sEPS}/gTS_{sEPS}	0.91 ± 0.01	–	–
Yield, sEPS	gVS_{sEPS}/gVS_{AGS}	0.23 ± 0.01	0.282 ± 0.010[a]	0.160 ± 0.004**
Yield, EPS	gTS_{EPS}/gTS_{AGS}	0.42 ± 0.01	–	–
PN, as BSA equivalent	$mgPN_{BSA}/gVS_{sEPS}$	617.8 ± 0.7	381.0 ± 5.0***	< detection limit of Bradford Standard Assay**
PS, as glucose equivalent	$mgPS_{Glu}/gVS_{sEPS}$	128.5 ± 3.1	138.0 ± 2.5***	122.5 **
PS, as alginate equivalent	$mgPS_{Alg}/gVS_{sEPS}$	942.7 ± 15.1	–	486.2 ± 22.3**
PN/PS_{Glu}	gPN_{BSA}/gPS_{Glu}	4.81 ± 0.05	2.76 ± 0.08***	–
PN/PS_{Alg}	gPN_{BSA}/gPS_{Alg}	0.66 ± 0.07	–	–
TN	mgN/gTS_{sEPS}	73.4 ± 0.1	74[a]	–
TP	mgP/gTS_{sEPS}	23.2 ± 0.2	28[a]	–

[a] (Felz et al., 2016), **(Lin et al., 2010), ***(Felz et al., 2019).

2.3. Thermogravimetric analysis (TGA)

Thermogravimetric (TG) and derivative thermogravimetric (DTG) analysis of dried sEPS and hydrogel were performed by means of a thermogravimetric analyser Q5000 TA Instruments heating the samples from room temperature up to 800 °C at 10 °C/min under a nitrogen flow rate of 100 mL/min. DTG signals were deconvolved using the peak fitting function in PeakFit®. The symmetrical Gaussian model which led to the highest R-square was chosen to fit the experimental data (Li et al., 2019). TGA was also used to determine the TS by maintaining the samples at 105 °C for 60 min and the VS by maintaining the samples at 560 °C for 60 min under nitrogen (N_2 flow: 100 mL/min).

2.4. Differential scanning calorimetry (DSC)

DSC experiments were performed with a Q1000 TA instrument by applying the same method carried out by Lotti et al, 2019a (Lotti et al., 2019b). The samples, sealed in aluminium pans, were equilibrated at 25 °C, cooled to −90 °C (cooling rate >30 °C/min), conditioned at −90 °C for 8 min to allow the complete freezing of the free water, and then heated up to 30 °C (heating rate = 1 °C/min) under a 50 mL/min flow of nitrogen. An empty sealed aluminium pan was used as reference. For each system, three different samples were prepared and analysed. The enthalpy of fusion of water was calculated through integration of the endothermic peak in the temperature range between −2.8 and 6.0 °C. The Free Water Index (FWI), a parameter commonly used to represent the amount of free and bound-freezable water contained in the samples, was calculated using the following equation:

$$FWI = \Delta H_{sample} / \Delta H_{freewater} \cdot 100 \quad (1)$$

Where ΔH_{sample} is the enthalpy change due to the fusion of the ice contained in the EPS hydrogel sample (J/g_{water}), experimentally determined from the DSC curve; $\Delta H_{freewater}$ (333.6 J/g) is the theoretical value of the specific fusion enthalpy of pure ice at 0 °C.

2.5. Rheology

Frequency sweep curves were collected by means of a TA Instruments Discovery Hybrid Rheometer HR-3 that works in controlled shear stress mode by using a plate-plate geometry (20 mm diameter, 400 μm gap), according to the same method carried out by previous work (Lotti et al., 2019b). The trend of the storage (G′) and loss (G″) moduli was studied in the linear viscoelastic range (LVR) of deformations (previously determined by means of amplitude sweep tests carried out at a constant frequency of 1Hz in a strain amplitude range between 0.01 and 20%) as a function of the oscillation frequency in the range 10^{-2}–10^{2} Hz; (the temperature was maintained at 25.00 ± 0.01 °C by means of a Peltier system). All the frequency sweep tests were carried out at a constant strain amplitude of 0.4%.

2.6. Statistical analysis

All measurements were performed in triplicates and the figures show the mean values and standard deviations.

3. Results and discussion

3.1. sEPS characterization

Table 1 reports the sEPS characterization. All the analysis were performed in triplicates. Regarding the TS determination for AGS and sEPS, the applied Standard Methods (APHA/AWWA/WEF, 2017) refer to keeping the sample at 105 °C for 24h in order to remove the water content. However, it is worth noting that TGA analysis for sEPS revealed that a weight loss up to 200–250 °C was mostly due to residual water evaporation, as outlined in a specific paragraph below. The presence of a portion of water that requires more thermal energy (i.e. from 105 °C to 200–250 °C) to be removed suggests that sEPS extracted from AGS present high water-holding capacity, as inferred by other authors (Nancharaiah and Sarvajith, 2019; Rosenzweig et al., 2012). As AGS are microorganisms embedded in a sEPS matrix, the same considerations drawn for sEPS are likely valid for AGS. Bearing in mind the above, the determination of TS and VS with standard methods (APHA/AWWA/-WEF, 2017) applied for conventional activated sludge leads to an overestimation of TS in the range 9–10% by mass (since water is not fully removed). The incorrect determination of TS results to an even higher overestimation of VS content in the range 9–10% by mass: the residual water content is fully removed in the muffle (550 °C for 2 h) and its weight is erroneously attributed to VS as calculated by subtracting the ash mass obtained in the muffle from the TS previously determined in the oven at 105 °C. Therefore, a modified protocol for TS determination should be applied for AGS as well as for biofilms in general, keeping the sample at 200–250 °C to ensure a complete water evaporation.

The yield of sEPS extraction was 0.23 gVS_{sEPS}/gVS_{AGS}, similar to literature results (Felz et al., 2016; Lin et al., 2010). It is worth nothing that since both the proteins (PN) and polysaccharides (PS) are determined by colorimetric methods, the numeric result is highly sensitive to the chosen standard. Therefore, the results of PN and PS should only be reported in a relative form as equivalents of the standard, as recently pointed out by Felz et al. (2019) (Felz et al., 2019).

The polysaccharides analysed using d-glucose as standard (PS_{Glu}) were 128.5 $mgPS_{Glu}/gVS_{sEPS}$, aligned with literature values, whereas PS_{Alg} were 942.7 $mgPS_{Alg}/gVS_{sEPS}$ significantly higher than other literature results (i.e. 486.2 $mgPS_{Alg}/gVS_{sEPS}$ by Lin et al., 2013 (Lin et al., 2013)). PS_{Alg} was 7.3 times greater than PS_{Glu}, thus suggesting an alginate-like composition of sEPS from AGS as reported by Lin et al. (2010) (Lin et al., 2010). It is possible to observe that the protein content is quite higher if compared to other studies (617.8 vs. 381 $mgPN_{BSA}/gVS_{sEPS}$ by Felz et al., 2019 (Felz et al., 2019)). Considering

Table 2
Elemental molar ratios of sEPS and hydrogels.

		N	H	P	S	Ca
		[N-mol/C-mol]	[H-mol/C-mol]	[P-mol/C-mol]	[S-mol/C-mol]	[Ca-mol/C-mol]
Hydrogels	**sEPS polymer**	0.154	1.688	0.019	0.013	0.002
	1% w/w sEPS	0.142	8.861	0.007	0.015	0.702
	2% w/w sEPS	0.141	2.979	0.006	0.014	0.411
	3% w/w sEPS	0.142	3.527	0.006	0.013	0.289
	5% w/w sEPS	0.148	2.649	0.006	0.015	0.206
	6% w/w sEPS	0.151	2.414	0.006	0.014	0.139
	7% w/w sEPS	0.147	2.072	0.006	0.014	0.149
	8% w/w sEPS	0.149	2.220	0.006	0.016	0.138
	10% w/w sEPS	0.149	2.092	0.007	0.016	0.138

that the TN concentrations was similar to literature results and given the difference between the PN concentration measured by colorimetric method and based on TN results (617.8 vs 504.1 mgPN/gVS_{sEPS}), it can be commonly used conversion factor of 6.25 gPN/gTN (Carvalho et al., 2013; Lotti et al., 2019a), the PN concentration calculated from the TN results would be equal to 504.1 mgPN/gVS_{sEPS} still higher, but closer, to reference literature values. Taking asserted that the sEPS in the present study contained some substances (e.g. humic acids, uronic acids, phenolic compounds, glucose, galacturonic acid, glucosamine) that could have positively interfered with the BCA assay, as reported in literature (Felz, 2019). Regarding the PN/PS ratio, it was registered 4.81 gPN_{BSA}/gPS_{Glu}, higher but in the same order of magnitude of literature value (2.76 gPN_{BSA}/gPS_{Glu}) (Felz et al., 2019). PN/PS was below 1 if it is calculated using PS as alginate equivalent, thus highlighting the dependence of this ratio on the standard and on the applied analytical method. In literature there are conflicting opinions about the relation between PN/PS of sEPS and structural stability of AGS. Most of the studies agree that PN are responsible for initial microbial aggregation and for maintenance of core structure and long-term stability of AGS (Adav and Lee, 2008; Erşan and Erguder, 2013; Franca et al., 2018; Xu et al., 2019; Zhu et al., 2012). On the other hand, some researchers found that the PS are more effective in contributing to structural stability of AGS (Tay et al., 2001). These contradictory results are attributable to the use of non-standardized analytical procedures for EPS extraction and analysis of components, thus limiting the possibility to compare the results of various studies (Franca et al., 2018). Furthermore, the colorimetric methods used to analyse the PS and PN contents are limited by both the variability of sample composition and by the wide variety of interfering substances that can affect the analyte estimation (Franca et al., 2018; Le and Stuckey, 2016).

3.2. Hydrogel formation and elemental analysis of sEPS and sEPS-based hydrogels

Compared to other hydrogel formation techniques based on the extrusion of hydrogel beads into a $CaCl_2$ cross-linker solution (Felz et al., 2016; Lin et al., 2013), in the present study the hydrogels were formed under controlled cross-linking kinetic conditions through a diffusion mechanism of Ca^{2+} ions passing through a 3.5 kDa MWCO dialysis bag into the sEPS aqueous solution (Campo et al., 2020a). Preliminary experiment showed that, especially for higher sEPS concentration, the hydrogel beads formed through an extrusion process were not homogeneous from the outer layer to the inner one due to the high rate of cross-linking process causing an instantaneous formation of a stiff outer hydrogel layer involving most of the EPS in solution. Therefore, the external layer appeared as little "gel bag" while the core was aqueous with EPS concentration much lower that the starting values (data not shown). In the present study the sEPS-based hydrogels formed by diffusion were characterized by a more homogeneous structure due to the lower kinetic of the diffusion compared to the extrusion method. Examining the results, hydrogel formation under controlled Ca^{2+}cross-linking kinetic conditions was feasible starting from sEPS concentrations as low as 1% w/w up to 10% w/w as gTS_{sEPS}/gWet-$Weight_{sEPS}$ (Fig. S1). This result highlight that, for the 1% w/w sEPS hydrogel, it is possible to store 99 gH_2O/g$_{sEPS}$. This water-holding capacity is typical of super absorbent polymers (SAPs) that are compounds able to absorb water and swell into hydrated matters equivalent to many times their original weight. SAPs crosslinked in a three-dimensional polymer network, are hydrogels that can be used in various industrial sectors such as chemical, paper, textile and agronomic to increase the water retention of soils (Kim et al., 2020; Lin et al., 2015; Milani et al., 2017; Po, 1994).

Elemental analysis of sEPS and sEPS-based hydrogels (Table 2) showed that the nitrogen/carbon molar ratio was maintained almost constant (0.154 N-mol/C-mol for sEPS vs. 0.146 ± 0.004 N-mol/C-mol as average value for hydrogels with 1–10% w/w sEPS), close to literature data (0.139 N-mol/C-mol by Felz, 2019 (Felz et al., 2019)). A noticeable increase of Ca/C molar ratio from sEPS to sEPS-based hydrogels (from 0.002 up to 0.702 Ca-mol/C-mol) suggested that during the hydrogel formation through the cross-linking process the inclusion of Ca^{2+} ions inside the tridimensional network of sEPS matrix occurred. Interestingly, the Ca-mol/C-mol ratio decreased from 0.702 mol Ca/C-mol down to 0.139 Ca-mol/C-mol for hydrogels formed with increasing concentration of sEPS from 1 to 6% w/w. Then, for hydrogels formed in the higher range of concentration 6–10% w/w of sEPS, the Ca/C molar ratio was almost constant close to 0.141 ± 0.005 Ca-mol/C-mol.

Focusing on this aspect, Fig. 1 shows Ca-mol/C-mol ratio as a function of sEPS concentration in sEPS-based hydrogels. It is evident that the Ca-mol/C-mol ratio decreases as sEPS concentration in hydrogels increases. Furthermore, there is a sEPS concentration in hydrogels (i.e. 6% w/w) above which the Ca-mol/C-mol ratio is almost constant. If we suppose that, after washing the hydrogel with water, all the Ca^{2+} revealed through elemental analysis (Table 2) is bound to the sEPS chains as crosslinker, the decrease of the Ca-mol/C-mol ratio in sEPS-

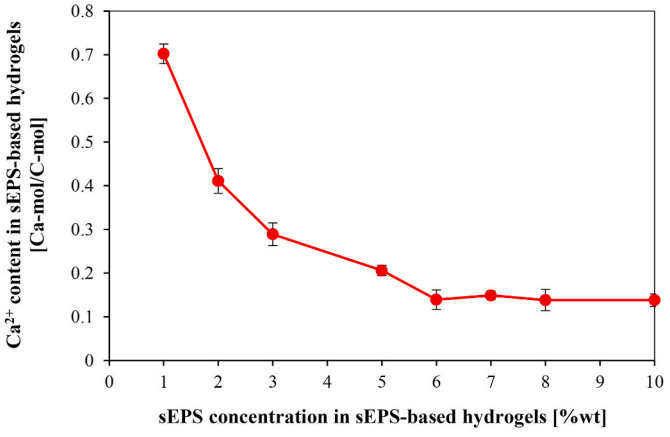

Fig. 1. Ca^{2+} content vs. sEPS concentration in sEPS-based hydrogels.

based hydrogels observed upon increasing the sEPS concentration in the same systems can be attributed to an excluded volume effect due to sEPS polymeric chains (Fixman, 1955). In detail, as the sEPS content rises, the space available for the crosslinking induced by the Ca^{2+} ions decreases, causing a reduction of the bound Ca^{2+} and, as a consequence, of the Ca-mol/C-mol ratio (Table 2 and Fig. 1). Another possible explaination of the observed phenomenon could likely be that the higher the sEPS concentration in hydrogels the higher is the probability to originate Ca-independent gelled clusters thus hindering the Ca^{2+} diffusion into the sEPS matrix and lowering the binding chances of Ca^{2+} with sEPS (Cao et al., 2020).

A complete characterization of the metals content in the sEPS is reported in e-supplementary data (Table S1).

3.3. FT-IR analysis of sEPS and sEPS-based hydrogels

FT-IR analysis revealed the functional groups involved in the complexation of Ca^{2+}. FT-IR spectra were collected on both pure sEPS and on a residue obtained by drying a hydrogel containing the 10% w/w of sEPS (Fig. 2a and S2). The FT-IR spectra analysis of sEPS and sEPS-based hydrogel revealed the principal functional groups belonging to proteins and polysaccharides (Fig. 2b). Observing the sEPS spectrum (Fig. 2, red line), similitudes were noticed with spectra of AGS fed with real wastewater (Lin et al., 2010, 2013; Schambeck et al., 2020).

After the formation of hydrogel through the cross-links between the sEPS molecules induced by the addition of Ca^{2+} ions, the FT-IR spectrum showed some changes in terms of peak-shifts. The most meaningful effects are observed for the peaks at 1540 cm^{-1}, that are attributable to Amide II (stretching of C–N and bending of N–H of proteins) and/or to alginate lyases (Lin et al., 2010), and for the peaks at 1240 cm^{-1} and 1047 cm^{-1} due respectively to C–OH stretching and to C–H in plane bending of polysaccharides. Therefore, this data suggest that the formation of Ca^{2+}-induced cross-linkings involved different functional groups, mainly polysaccharides, maybe through the formation of supramolecular structures like to the well-known egg-boxes ones, typical of alginates and alginate-like polymers (Cao et al., 2020). These observations indicate that the polysaccharides play a fundamental role in the Ca^{2+} complexation mechanism, whereas the proteins are marginally

A

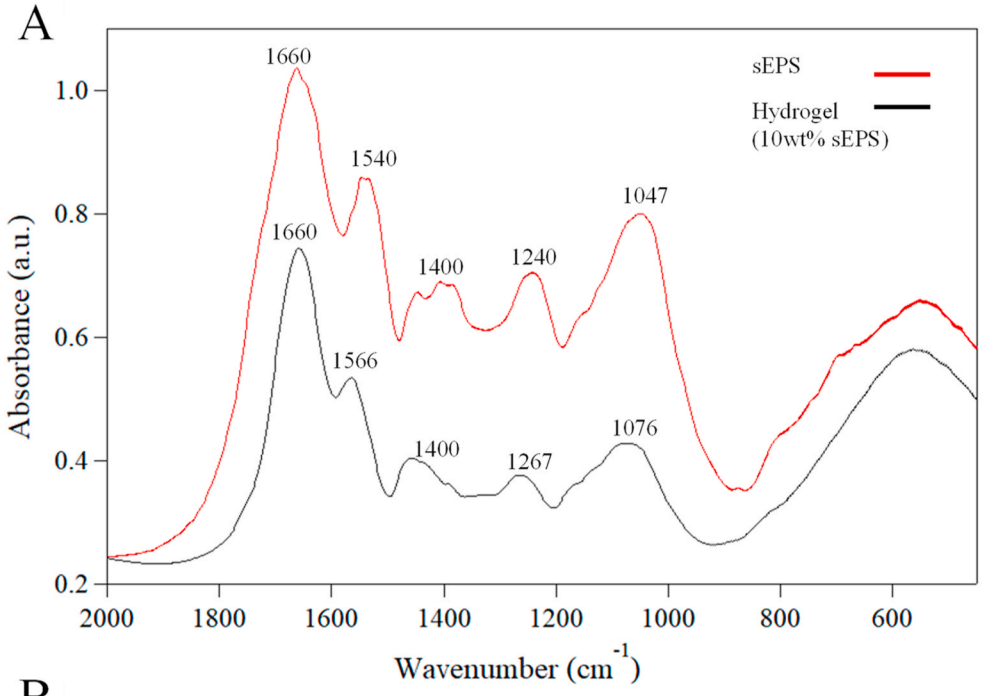

B

Frequencies [cm^{-1}]	Assignments	Refs
1660	Carboxyl group O-C-O (asymmetric stretch vibration) Proteins Amide I	(Silverstein et al., 2005; Lin et al., 2018)
1540	Proteins Amide II Alginate lyase	(Gallagher, 2009; Lin et al., 2010)
1400	Carboxyl group O-C-O (symmetric stretch vibration) Proteins Amide III	(Pereira et al., 2003; Silverstein et al., 2005; Gallagher, 2009; Sellimi et al., 2015)
1240	C-OH stretching of polysaccharides	(Silverstein et al., 2005)
1047	C-H in plane bending of polysaccharides	(Silverstein et al., 2005)

Fig. 2. a) FT-IR spectra of sEPS and hydrogels containing 10% w/w of sEPS; b) assignments of the main functional groups.

involved during cross-linking process for hydrogel formation as no peak-shifts were observed for Amide I (1660 cm^{-1}) and Amide III (1400 cm^{-1}) functional groups (Fig. 2a).

Moreover, it should be also stressed that, as a more complex aggregative structure of sEPS has been recently reported in literature (Felz et al., 2020b; Lin et al., 2018). It involves the presence of glycosylated amyloid and sulphated glycosaminoglycans (GAGs) both linked with proteins; then, during the cross-linking process it is reasonable to suppose that also proteins linked to polysaccharidic chains (i.e. glycosylated amyloid or glycosaminoglycans) can be indirectly involved. This likely accounts for the shift of the peak of amide II observed after the addition of Ca^{2+}.

3.4. Thermogravimetric analysis of sEPS and sEPS-based hydrogels

TG and DTG analysis have been performed for dried sEPS and hydrogel samples (Campo et al., 2020a). The analysis of both the TG and DTG curves of dried sEPS revealed three main stages of thermal decomposition of samples (Fig. S3) (Li et al., 2019): i) evaporation of residual moisture, between 200 and 250 °C, that was not possible to remove after oven-drying at 105 °C for 48 h (weight loss close to 5.6% w/w); ii) organic matter volatilization in the range 200–535 °C); iii) decomposition of minerals present in sEPS in the range 535–800 °C. After the deconvolution of the peaks in the DTG curve of sEPS in the range of temperature between 200 and 500 °C (Fig. 3a), three main contributions are detectable (Bach and Chen, 2017): i) low thermal resistant proteins (PN I) were likely associated to the first peak close to 270 °C; ii) high thermal resistant polysaccharides (PS), such as alginate-like polysaccharides (Li et al., 2019), were likely associated to the second peak close to 290 °C; iii) high thermal resistant proteins (PN II) were likely associated to the third peak close to 300 °C. By studying the deconvolution of the DTG curves of hydrogel in the same range of temperature (i.e. 200-500 °C) (Fig. 3b), it is possible, also in this case, to observe at least three distinct contributions. The first one, close to 270 °C, is associable to the low thermal resistant proteins (PN I). This peak is similar in intensity and aligned to the first peak in the DTG curve of sEPS sample (Fig. 3a), thus suggesting that PN I are not involved in the cross-linking reaction. The second peak, close to 300 °C, might be attributed to the high thermal resistant proteins (PN II). Also in this case, this peak is similar in intensity and aligned to the third peak in the DTG curve of sEPS sample (Fig. 3a), thus indicating that PN II are not involved in the cross-linking reaction. In summary, by comparing the DTG curves of dried EPS and of the hydrogel (Fig. 3a vs 3b), it is reasonable to assert that both PN I and PN II do not undergo substantial structural modifications during the cross-linking reaction as indicated by the signal and the position of the relative peaks. The persistence of the position of the DTG peak for both the low thermal (PN I) and the high thermal resistant proteins (PN II, Fig. 3), is consistent with the idea that those proteins do not participate to the formation of Ca^{2+} cross-links between the sEPS chains. This datum is also supported by the third peak of the DTG curve of hydrogel close to 350 °C, labeled as PS (Fig. 3b), attributable to the high thermal resistant polysaccharides such as alginates (Li et al., 2019). After the addition of Ca^{2+}, this peak was shifted toward higher temperature values. The shift magnitude is almost 60 °C in comparison to the DTG curve of sEPS (Fig. 3a). This was likely due to the high energy needed to thermally decompose the polysaccharides that are strongly cross-linked by Ca^{2+} in the tridimensional hydrogel network. These results corroborate the FT-IR analysis discussed previously. In fact, as from DTG analysis proteins seem do not contribute meaningfully to cross-linking (Fig. 3), the observed peak-shifts at 1540 cm^{-1} and 1400 cm^{-1} in the FT-IR spectra (Fig. 2) are not due to proteins but they are likely attributable to polysaccharidic functional groups (i.e. alginate-like polymers). Finally, additional contributions between 400 and 500 °C in the DTG curves of both sEPS and sEPS-based hydrogel are likely associable to the thermal decomposition of the EPS lipid fraction (Bach and Chen, 2017).

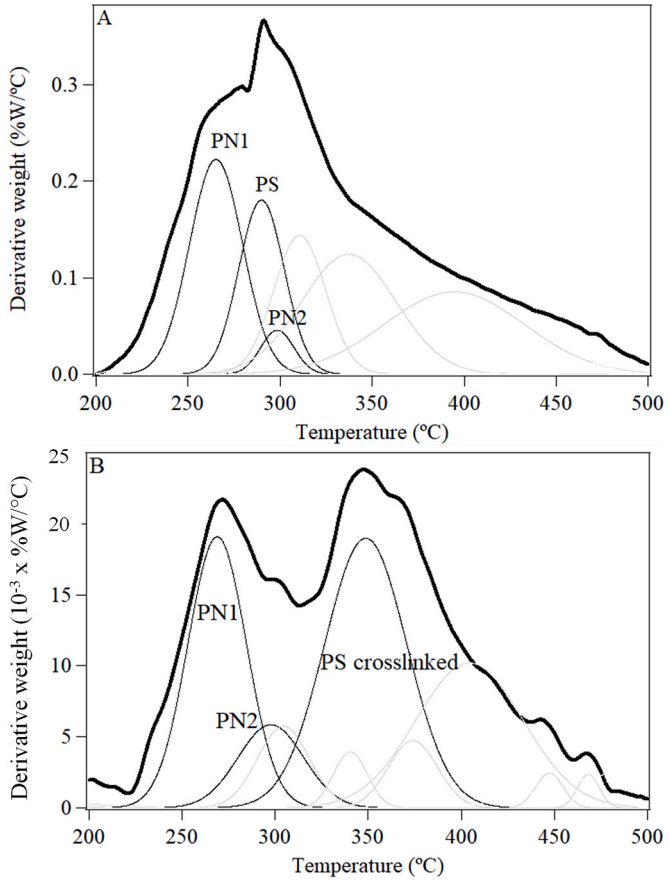

Fig. 3. Derivative thermogravimetric (DTG) curves (bold lines) and deconvolution of DTG signals of sEPS (a) and sEPS-based hydrogels (b).

3.5. DSC analysis of sEPS-based hydrogels

DSC analysis have been conducted to estimate the entity of the interactions between the water and the sEPS-based hydrogels tridimensional network, similarly to what has been reported in literature for hydrogels generated with EPS extracted from anammox bacteria (Lotti

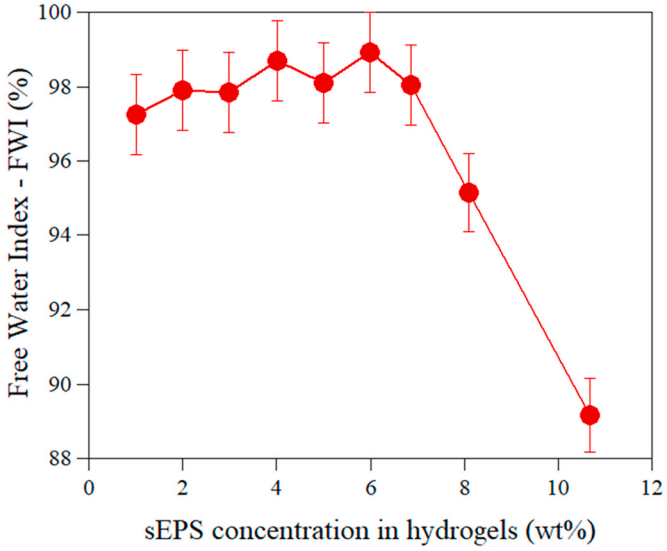

Fig. 4. Free Water Index vs. sEPS concentration in hydrogels.

et al., 2019b). Fig. 4 shows the trend of the FWI as a function of the sEPS content into the hydrogels. As seen in the graph, for sEPS concentrations between 2% w/w and 6% w/w, the FWI remains almost unvaried (97–98%). By further increasing the sEPS content, the amount of not freezable water (that is the fraction of water that, being strongly bound to the polymer network doesn't freeze even at temperatures below 0 °C) increases up to 11% w/w.

3.6. Rheology of sEPS-based hydrogels

The mechanical properties of a series of gels have been investigated as a function of the sEPS concentration while maintaining the concentration of $CaCl_2$ cross-linking solution constantly equal to 2.5% w/w. Fig. S3 shows the G' (storage modulus) and the G" (loss modulus), at a constant strain of 0.4%, as a function of the frequency for all the investigated samples. It was observed that G'≫G″ for all the investigated systems and, in the explored frequency range, no crossover between the G' and G" curves were registered. This indicates first that all the investigated systems show a solid-like behavior and, thus, are characterized by an infinite relaxation time; moreover, on this basis they can be all rigorously classified as gels (Almdal et al., 1993).

Fig. 5 shows the G′ values at 1Hz vs the sEPS % w/w. There is a discontinuity in the slope of the curve that drastically increases for sEPS concentration higher than 4% w/w, indicating that above this threshold value, the progressive extension of the 3D network occurs more rapidly as the sEPS concentration increases too. The same test was carried out for Calcium-Alginate hydrogels, and, in that case, it was not observed any discontinuity in the G' values that resulted in linear correlation with alginate % w/w (data not shown).

In order to better understand the mechanism of sEPS-based hydrogel formation, Fig. 6 shows a log/log plot of the values of G′ at 1Hz vs the concentration of sEPS. The fit of the experimental data indicates that the value of G′ scales following a power-law characterized by a fit of the hydrogels % w/w of sEPS (Fig. 6a) and alginate (Fig. 6b) vs the G' modulus, results in an exponent value ("n" value) close to 2.0 for both the hydrogels. On the basis of the De Gennes theory describing the behavior of polymers in solution (De Gennes, 1976; Pääkko et al., 2007), this value indicates that the expansion of the sEPS network occurs through a percolation mechanism and in a similar way for sEPS and alginate thus further confirming the similarity of behavior of sEPS with alginate polymers (Lin et al., 2010). This finding represents a first answer to the open question about sEPS-based hydrogel mechanism of formation (Felz et al., 2020a). The "percolative model", commonly

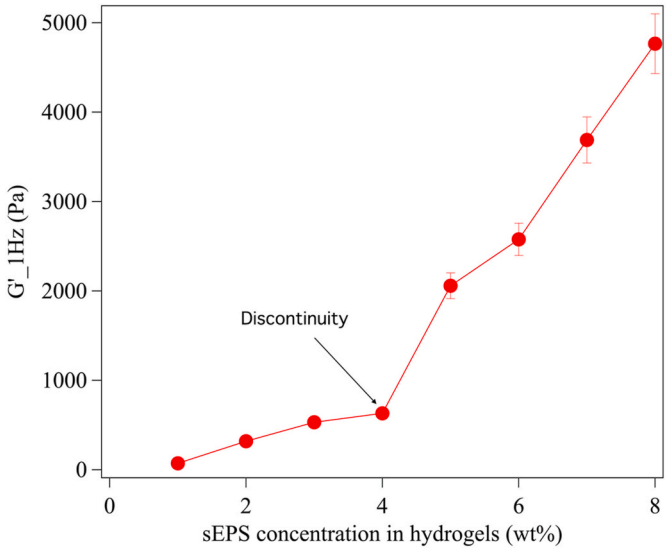

Fig. 5. Storage module (G′) vs. sEPS concentration in hydrogels.

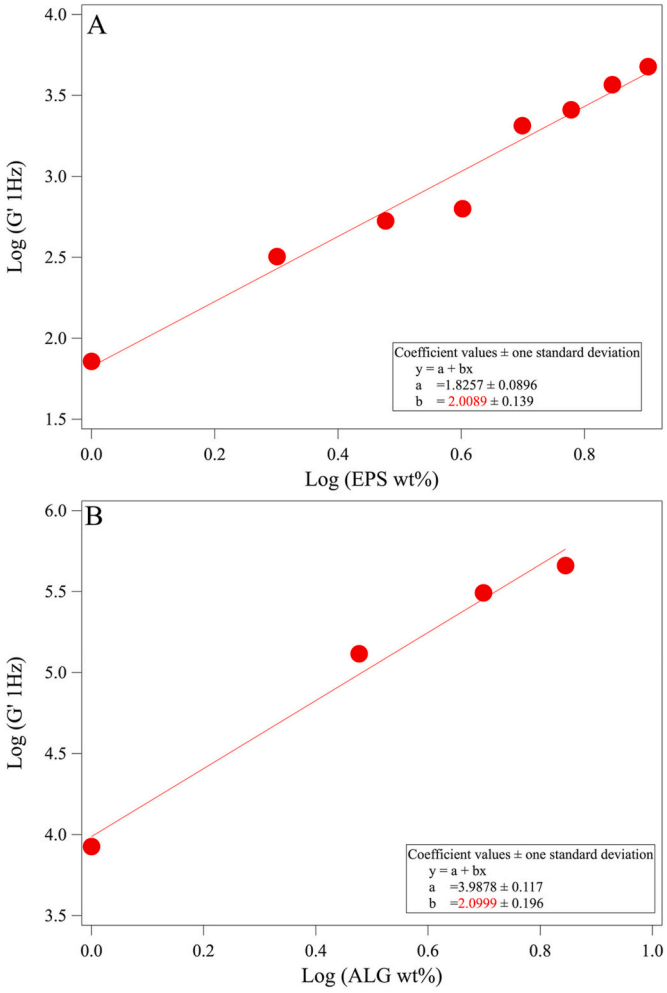

Fig. 6. Log G′ vs. Log sEPS hydrogel concentration (a); Log G′ vs. Log Alginate hydrogel concentration (b).

adopted to describe the formation of chemically cross-linked networks, indicates that first the formation of clusters composed by sEPS oligomers occurs, followed by their interconnection that originates an"infinite" tridimensional network through the whole volume of the sample.

On these bases, and considering the results of the FT-IR and TGA investigations, it is reasonable to suppose that for sEPS hydrogels the crosslinking are formed as "egg-boxes", as typical of alginate/Ca cross-linked networks (Braccini and Pérez, 2001; Cao et al., 2020) and the extension of the network formed through these crosslinks occurs through a "percolative model", that is the same also for alginate hydrogels.

3.7. Effects of sEPS hydrogel formation mechanisms on AGS structural stability

AGS is known as a biofilm made of microorganisms embedded in an EPS gelatinous matrix (Lin et al., 2010; Seviour et al., 2009a, 2009b). As shown previously in Table 1, this matrix is mainly composed of proteins, considered responsible for granules structural stability and adhesion of microorganisms (Flemming and Wingender, 2010), and polysaccharides that interacting and binding with proteins through hydrogen bond contribute to the gel-structure of EPS (Li et al., 2020; Lin et al., 2018). It should be stressed that the sEPS extraction protocol applied in this study might alter the original sEPS structure or some components but the relationship between the main sEPS components (i.e. proteins and polysaccharides) might be maintained, as also reported by (Li et al.,

2020). Therefore, all the considerations drawn in this work about the extracted sEPS and hydrogel properties might be valid also in their original location inside the pristine AGS.

Bearing in mind the above, the implications of the obtained results can be, at least, twofold:

- Understanding the key-role of sEPS and sEPS-based hydrogel in AGS formation and structural stability.
- Understanding the possible applications of the extracted sEPS and sEPS-based hydrogels as recovered resources, according to their physico-chemical and rheological properties.

3.7.1. The key-role of sEPS and sEPS-based hydrogel in AGS formation and structural stability

In literature, recent rheological sweep tests revealed that, after sEPS extraction from AGS, the residual AGS-pellet showed a crossover point of G′ and G" passing from elastic behaviour (G'>G″) to viscous behaviour (G'<G″) at lower strain (3–4%) compared to the original AGS (10–11% strain), as reported by Li et al. (2020) (Li et al., 2020). They consider that this evidence could be likely due to a shifting of mechanical properties dominance from elastic (solid-like) to viscous (liquid-like) after sEPS extraction, thus confirming that sEPS confer structural stability to AGS and are crucial both during granules formation and in the long-term granules' structural maintenance (Lin et al., 2018). Frequency sweep tests in the LVR conducted at a constant strain amplitude of 0.5% for AGS and sEPS, anticipated the solid-like behaviour of AGS and sEPS (G'>G") suggesting the gel-like structure (Caggioni et al., 2007; Lin et al., 2018).

Compared to recent studies that reported characterizations and rheological test of sEPS extracted from AGS (Li et al., 2020; Lin et al., 2018; Wang et al., 2021), the real novelty of the present study is represented by the characterization of sEPS-based hydrogels in order to understand the properties of sEPS-based hydrogels naturally present in AGS structure and how they can influence AGS stability.

As reported above, in the present study the frequency sweep test revealed that G'≫G″ in the explored frequency range for all the sEPS-based hydrogels. This confirmed that sEPS-based hydrogels that normally constitute aerobic granules, confer stiffness and mechanical strength to AGS structure. Furthermore, the increasing slopes of G' and G" curves in the frequency sweep tests(Fig. S4) indicate that the sEPS-based hydrogels are physically entangled/crosslinked (Grillet et al., 2012).

By combining the rheological results with the FT-IR data, it is possible to assert that the major contribution to mechanical strength and stability of AGS structure is attributable to sEPS and sEPS-based hydrogels. A key role in AGS formation and maintenance of stability is due to the polysaccharidic component of sEPS that strongly contribute to cross-linking process thus forming sEPS-based hydrogels when put in contact with Ca^{2+} ions (Fig. 2). These hydrogels have peculiar thermodynamic and mechanical properties that confer stiffness to AGS. Furthermore, the recently discovered existence of GAGs-like polysaccharides covalently bound to proteins in sEPS might be another factor increasing AGS structural stability (Felz et al., 2020b).

3.7.2. Remarks on the sEPS recovery and possible applications

Currently, the extraction of sEPS from waste AGS is considered as a virtuous pathway in the logic of water resource recovery facilities (WRRFs) (Duque et al., 2021; Kehrein et al., 2020; Kisser et al., 2020; ROYAL HASKONINGDHV, 2020). The first direct effect of sEPS recovery from waste AGS is represented by a significant reduction of excess sludge disposal whose costs represent one of the greatest incidence of OPEX costs for a wastewater treatment company (Wei et al., 2003). The structural and non-structural EPS yields extraction from AGS account for 23% and 19% w/w, respectively. The sEPS are totally recovered thus ensuring a 23% less of waste sludge disposal. The non-structural EPS can be considered as a liquid stream containing organic matter, expressed as COD, that might be recirculated at the head of the WWTP. The biodegradable fraction (bCOD) of non-structural EPS will be metabolized by microorganisms in the biological reactor thus resulting in the production of additional waste sludge the higher the observed yield factor of the biomass. Also, the particulate inert fraction (piCOD) of non-structural EPS will result in a further production of waste sludge. Bearing in mind the above, the effective quantification of reduction of excess sludge disposal will be somewhere in between 23% and 42%, considering that the two major factors related to minimization of waste sludge production from the non-structural EPS are: i) low observed yield factor of biomass; ii) low piCOD. The theoretical lower limit (23%) corresponds to the extraction yield of recovered sEPS if all the 19% w/w of non-structural EPS is composed by inert particulate substances (piCOD). The theoretical upper limit (42%) will result if all the 19% w/w of non-structural EPS is composed by inert soluble substances.

Other putative open questions related to EPS extraction are the influence on the dewaterability (van Der Roest et al., 2015) and on the aerobic/anaerobic biodegradability of the residual sludge (Guo et al., 2020a, 2020b). However, to date no direct experimental studies are available in literature about these topics, therefore further research is needed to unravel these aspects.

The water-holding capacity up to 99 gH_2O/g_{sEPS} for 1% w/w sEPS-based hydrogel (paragraph 3.2) suggests that these kind of hydrogels might be used as raw materials, or in combination with other materials, in chemical, paper and textile sectors (as coating agent) as well as soil-enhancer/conditioner in agronomic sector to increase the water-holding capacity of soils affected by water scarcity and/or to reduce/control the leakage of fertilizers in plantations (Amorim de Carvalho et al., 2021; Lin et al., 2015; Milani et al., 2017; Pronk et al., 2017).

Given that to date many of the sEPS properties are still unknown, it is not possible to perform an accurate analysis of the market value of this recovered resource. Undoubtedly, given the growing number of scientific publications about EPS recovery and the recent discovered physico-chemical properties of EPS, the extraction of sEPS from AGS might be a potential future product recovery route at full-scale (Kehrein et al., 2020). To date the only two full-scale sEPS recovery plants are located in The Netherlands thanks to public-private initiatives that enable the sustainable recovery of sEPS supporting the CAPEX/OPEX costs of the extraction chain (van Der Roest et al., 2015). The first extraction plant was started in Zutphen in 2019 and produce up to 400 ton/year of sEPS, whereas the second plant was started in EPE in 2020 and produce up to 100 ton/year of sEPS. The estimated extraction yield of both plants was close to 22.5% (DHV-Nereda®Plants, 2021; van Leeuwen et al., 2018). The reported results of this study as well as of many of the recent studies about sEPS, suggest investing in the recovery of sEPS from AGS as a resource and in the research for its sustainable and innovative applications.

4. Conclusions

- sEPS were extracted from AGS with a 0.23 gVS_{sEPS}/gVS_{AGS} yield factor.
- Hydrogel formation was feasible starting from a 1% w/w up to 10% w/w as gTS_{sEPS}/gWW_{sEPS}, upon controlled cross-linking with Ca^{2+}, thus holding up to 99 gH_2O/g_{sEPS}.
- FT-IR and DTG data suggest that the crosslinks inside the sEPS network involve mainly the polysaccharidic fraction, reasonably through the formation of "egg-box" crosslinking structures.
- sEPS-based hydrogels have solid-like behaviour (G'≫G″). The formation of the sEPS 3D network involves first, the formation of clusters composed by sEPS oligomers and then their connection through the whole volume of the sample with the formation of a tridimensional network by means of a percolative mechanism. This outcome is a novelty in sEPS characterization and the percolative mechanism was observed for both sEPS-based and alginate hydrogels

used as reference model further confirming that, also for sEPS-based hydrogel, polysaccharides play a primary role in the network formation and spatial expansion.

Author contribution statement

Riccardo Campo: Conceptualization, Methodology, Investigation, Writing – original draft, Writing – review & editing. Emiliano Carretti: Conceptualization, Methodology, Resources, Writing – review & editing. Claudio Lubello: Resources, Writing – review & editing, Supervision, Project administration, Funding acquisition. Tommaso Lotti: Conceptualization, Methodology, Resources, Writing – review & editing, Supervision, Project administration, Funding acquisition.

Declaration of competing interest

The authors declare that they have no known competing financial interests or personal relationships that could have appeared to influence the work reported in this paper.

Data availability

The authors do not have permission to share data.

Acknowledgements

This research was funded by: ROP-ESFR Toscana 2014–2022 - IDRO. SMART project (CUP: 3647.04032020.157000040). A special thanks to "MP Architettura Design" for its contribution in 3D printing of supports for hydrogel formation.

Appendix A. Supplementary data

Supplementary data to this article can be found online at https://doi.org/10.1016/j.jenvman.2022.116247.

References

Adav, S.S., Lee, D.-J., 2008. Extraction of extracellular polymeric substances from aerobic granule with compact interior structure. J. Hazard Mater. 154, 1120–1126. https://doi.org/10.1016/j.jhazmat.2007.11.058.

Almdal, K., Dyre, J., Hvidt, S., Kramer, O., 1993. Towards a phenomenological definition of the term 'gel'. Polymer gels and networks 1 (1), 5–17. https://doi.org/10.1016/0966-7822(93)90020-I.

Amin Vieira da Costa, N.P., Libardi, N., Ribeiro da Costa, R.H., 2022. How can the addition of extracellular polymeric substances (EPS)-based bioflocculant affect aerobic granular sludge (AGS)? J. Environ. Manag. 310, 114807. https://doi.org/10.1016/j.jenvman.2022.114807.

Amorim de Carvalho, C. de, Ferreira dos Santos, A., Tavares Ferreira, T.J., Sousa Aguiar Lira, V.N., Mendes Barros, A.R., Bezerra dos Santos, A., 2021. Resource recovery in aerobic granular sludge systems: is it feasible or still a long way to go? Chemosphere 274, 129881. https://doi.org/10.1016/j.chemosphere.2021.129881.

APHA/AWWA/WEF, 2017. Standard methods for the examination of water and wastewater. In: American Public Health Association, Washingto, DC, USA, 23rd ed. Am. Public Heal. Assoc. Washingto, DC, USA.

Bach, Q.V., Chen, W.H., 2017. A comprehensive study on pyrolysis kinetics of microalgal biomass. Energy Convers. Manag. 131, 109–116. https://doi.org/10.1016/j.enconman.2016.10.077.

Braccini, I., Pérez, S., 2001. Molecular basis of Ca2+-induced gelation in alginates and pectins: the egg-box model revisited. Biomacromolecules 2 (4), 1089–1096. https://doi.org/10.1021/bm010008g.

Caggioni, M., Spicer, P.T., Blair, D.L., Lindberg, S.E., Weitz, D.A., 2007. Rheology and microrheology of a microstructured fluid: the gellan gum case. J. Rheol. 51 (5), 851–865. https://doi.org/10.1122/1.2751385.

Campo, R., Pagliaccia, B., Carretti, E., Berti, D., Caffaz, S., Lubello, C., Lotti, T., 2020a. Analysis of formation and characterization of hydrogels originated from structural extracellular polymeric substances (sEPS) extracted from aerobic granular sludge (AGS). In: IWA Biofilms 2020 Virtual Conference: Emerging Trends and Developments in Biofilm Processes.

Campo, R., Sguanci, S., Caffaz, S., Mazzoli, L., Ramazzotti, M., Lubello, C., Lotti, T., 2020b. Efficient carbon, nitrogen and phosphorus removal from low C/N real domestic wastewater with aerobic granular sludge. Bioresour. Technol. 305, 122961. https://doi.org/10.1016/j.biortech.2020.122961.

Cao, L., Lu, W., Mata, A., Nishinari, K., Fang, Y., 2020. Egg-box model-based gelation of alginate and pectin: a review. Carbohydr. Polym. 242, 116389. https://doi.org/10.1016/j.carbpol.2020.116389.

Carvalho, F., Prazeres, A.R., Rivas, J., 2013. Cheese whey wastewater: characterization and treatment. Sci. Total Environ. 445, 385–396. https://doi.org/10.1016/j.scitotenv.2012.12.038.

De Gennes, P.G., 1976. Scaling theory of polymer adsorption. J. Phys. 44 (7), 241–246. https://doi.org/10.1051/jphys:019760037012014450.

de Graaff, D.R., Felz, S., Neu, T.R., Pronk, M., van Loosdrecht, M.C.M., Lin, Y., 2019. Sialic acids in the extracellular polymeric substances of seawater-adapted aerobic granular sludge. Water Res. 155, 343–351. https://doi.org/10.1016/J.WATRES.2019.02.040.

DHV-Nereda®Plants, 2021. AGS wastewater treatment plants [WWW Document]. URL. https://www.royalhaskoningdhv.com/en-gb/nereda/nereda-plants-a-to-z. accessed 11.4.21.

Dreywood, R., 1946. Qualitative test for carbohydrate. Material. Ind. Eng. Chem. - Anal. Ed. 18 (8), 499. https://doi.org/10.1021/i560156a015.

Duque, A.F., Campo, R., Rio, A.V. Del, Amorim, C.L., 2021. Wastewater valorization: practice around the world at pilot-and full-scale. Int. J. Environ. Res. Publ. Health 18 (18), 9466. https://doi.org/10.3390/ijerph18189466.

Erşan, Y.T., Erguder, T.H., 2013. The effects of aerobic/anoxic period sequence on aerobic granulation and COD/N treatment efficiency. Bioresour. Technol. 148, 149–156.

Felz, S., 2019. Structural Extracellular Polymeric Substances from Aerobic Granular Sludge. (Doctoral dissertation, Delft University of Technology).

Felz, S., Al-Zuhairy, S., Aarstad, O.A., van Loosdrecht, M.C.M., Lin, Y.M., 2016. Extraction of structural extracellular polymeric substances from aerobic granular sludge. JoVE (115), e54534. https://doi.org/10.3791/54534.

Felz, S., Kleikamp, H., Zlopasa, J., van Loosdrecht, M.C.M., Lin, Y., 2020a. Impact of Metal Ions on Structural EPS Hydrogels from Aerobic Granular Sludge, 2. Biofilm, p. 100011. https://doi.org/10.1016/j.bioflm.2019.100011.

Felz, S., Neu, T.R., van Loosdrecht, M.C.M., Lin, Y., 2020b. Aerobic granular sludge contains Hyaluronic acid-like and sulfated glycosaminoglycans-like polymers. Water Res. 169, 115291. https://doi.org/10.1016/j.watres.2019.115291.

Felz, S., Vermeulen, P., van Loosdrecht, M.C.M., Lin, Y.M., 2019. Chemical Characterization Methods for the Analysis of Structural Extracellular Polymeric Substances (EPS). Water Research 157, 201–208.

Fixman, M., 1955. Excluded volume in polymer chains. J. Chem. Phys. 23 (9), 1656–1659. https://doi.org/10.1063/1.1742405.

Flemming, H.-C., Wingender, J., 2010. The biofilm matrix. Nat. Rev. Microbiol. 8, 623–633.

Franca, R.D.G., Pinheiro, H.M., van Loosdrecht, M.C.M., Lourenço, N.D., 2018. Stability of aerobic granules during long-term bioreactor operation. Biotechnol. Adv. 36 (1), 228–246. https://doi.org/10.1016/j.biotechadv.2017.11.005.

Grillet, A.M., Wyatt, N.B., Gloe, L.M., 2012. Polymer gel rheology and adhesion. Rheology 3, 59–80.

Guo, H., Felz, S., Lin, Y., van Lier, J.B., de Kreuk, M., 2020a. Structural extracellular polymeric substances determine the difference in digestibility between waste activated sludge and aerobic granules. Water Res. https://doi.org/10.1016/j.watres.2020.115924.

Guo, H., van Lier, J.B., de Kreuk, M., 2020b. Digestibility of waste aerobic granular sludge from a full-scale municipal wastewater treatment system. Water Res. 173, 115617. https://doi.org/10.1016/j.watres.2020.115617.

Karakas, I., Sam, S.B., Cetin, E., Dulekgurgen, E., Yilmaz, G., 2020. Resource recovery from an aerobic granular sludge process treating domestic wastewater. J. Water Proc. Eng. 34, 101148.. https://doi.org/10.1016/j.jwpe.2020.101148.

Kehrein, P., Van Loosdrecht, M., Osseweijer, P., Garfí, M., Dewulf, J., Posada, J., 2020. A critical review of resource recovery from municipal wastewater treatment plants-market supply potentials, technologies and bottlenecks. Environ. Sci. Water Res. Technol. 6 (4), 877–910. https://doi.org/10.1039/c9ew00905a.

Kim, N.K., Lin, R., Bhattacharyya, D., van Loosdrecht, M.C.M., Lin, Y., 2022. Insight on how biopolymers recovered from aerobic granular wastewater sludge can reduce the flammability of synthetic polymers. Sci. Total Environ. 805, 150434 https://doi.org/10.1016/J.SCITOTENV.2021.150434.

Kim, N.K., Mao, N., Lin, R., Bhattacharyya, D., van Loosdrecht, M.C.M., Lin, Y., 2020. Flame retardant property of flax fabrics coated by extracellular polymeric substances recovered from both activated sludge and aerobic granular sludge. Water Res. 170, 115344. https://doi.org/10.1016/j.watres.2019.115344.

Kisser, J., Wirth, M., De Gusseme, B., Van Eekert, M., Zeeman, G., Schoenborn, A., Vinnerås, B., Finger, D.C., Kolbl Repinc, S., Bulc, T.G., Bani, A., Pavlova, D., Staicu, L.C., Atasoy, M., Cetecioglu, Z., Kokko, M., Haznedaroglu, B.Z., Hansen, J., Istenič, D., Canga, E., Malamis, S., Camilleri-Fenech, M., Beesley, L., 2020. A review of nature-based solutions for resource recovery in cities. Blue-Green Syst 2 (1), 138–172. https://doi.org/10.2166/bgs.2020.930.

Le, C., Stuckey, D.C., 2016. Colorimetric measurement of carbohydrates in biological wastewater treatment systems: a critical evaluation. Water Res. 94, 280–287. https://doi.org/10.1016/j.watres.2016.03.008.

Li, X., Lin, S., Hao, T., Khanal, S.K., Chen, G., 2019. Elucidating pyrolysis behaviour of activated sludge in granular and flocculent form: reaction kinetics and mechanism. Water Res. 162, 409–419. https://doi.org/10.1016/j.watres.2019.06.074.

Li, Z., Lin, L., Liu, X., Wan, C., Lee, D.J., 2020. Understanding the role of extracellular polymeric substances in the rheological properties of aerobic granular sludge. Sci. Total Environ. 705, 135948. https://doi.org/10.1016/j.scitotenv.2019.135948.

Lin, Y., de Kreuk, M., van Loosdrecht, M.C.M.M., Adin, A., 2010. Characterization of alginate-like exopolysaccharides isolated from aerobic granular sludge in pilot-plant. Water Res. 44, 3355–3364. https://doi.org/10.1016/j.watres.2010.03.019.

Lin, Y., Reino, C., Carrera, J., Pérez, J., van Loosdrecht, M.C.M., 2018. Glycosylated amyloid-like proteins in the structural extracellular polymers of aerobic granular sludge enriched with ammonium-oxidizing bacteria. Microbiol. 7 (6), e00616. https://doi.org/10.1002/MBO3.616.

Lin, Y.M., Nierop, K.G.J., Girbal-Neuhauser, E., Adriaanse, M., van Loosdrecht, M.C.M., 2015. Sustainable polysaccharide-based biomaterial recovered from waste aerobic granular sludge as a surface coating material. Sustain. Mater. Technol. 4, 24–29. https://doi.org/10.1016/j.susmat.2015.06.002.

Lin, Y.M., Sharma, P.K., van Loosdrecht, M.C.M., 2013. The chemical and mechanical differences between alginate-like exopolysaccharides isolated from aerobic flocculent sludge and aerobic granular sludge. Water Res. 47, 57–65.

Lin, Y.M., Wang, L., Chi, Z.M., Liu, X.Y., 2008. Bacterial alginate role in aerobic granular bio-particles formation and settleability improvement. Separ. Sci. Technol. 43, 1642–1652. https://doi.org/10.1080/01496390801973805.

Liu, W., Zhang, J., Jin, Y., Zhao, X., Cai, Z., 2015. Adsorption of Pb(II), Cd(II) and Zn(II) by extracellular polymeric substances extracted from aerobic granular sludge: efficiency of protein. J. Environ. Chem. Eng. 3, 1223–1232. https://doi.org/10.1016/j.jece.2015.04.009.

Lotti, T., Carretti, E., Berti, D., Martina, M.R., Lubello, C., Malpei, F., 2019a. Extraction, recovery and characterization of structural extracellular polymeric substances from anammox granular sludge. J. Environ. Manag. 236, 649–656. https://doi.org/10.1016/j.jenvman.2019.01.054.

Lotti, T., Carretti, E., Berti, D., Montis, C., Del Buffa, S., Lubello, C., Feng, C., Malpei, F., 2019b. Hydrogels formed by anammox extracellular polymeric substances: structural and mechanical insights. Sci. Rep. 9 (1), 1–9. https://doi.org/10.1038/s41598-019-47987-8.

Lowry, O.H., Rosebrough, N.J., Farr, A.L., Randall, R.J., 1951. Protein measurement with the folin-phenol reagent. J. Biol. Cemistry 193, 265–275. https://doi.org/10.1016/0304-3894(92)87011-4.

Milani, P., França, D., Balieiro, A.G., Faez, R., 2017. Polymers and its applications in agriculture. Polímeros 27, 256–266.

Nancharaiah, Y.V., Sarvajith, M., 2019. Aerobic granular sludge process: a fast growing biological treatment for sustainable wastewater treatment. Curr. Opin. Environ. Sci. Heal. 12, 57–65. https://doi.org/10.1016/j.coesh.2019.09.011.

Pääkko, M., Ankerfors, M., Kosonen, H., Nykänen, A., Ahola, S., Österberg, M., Ruokolainen, J., Laine, J., Larsson, P.T., Ikkala, O., Lindström, T., 2007. Enzymatic hydrolysis combined with mechanical shearing and high-pressure homogenization for nanoscale cellulose fibrils and strong gels. Biomacromolecules 8 (6), 1934–1941. https://doi.org/10.1021/bm061215p.

Po, R., 1994. Water-absorbent polymers: a patent survey. J. Macromol. Sci. Rev. Macromol. Chem. Phys. 34 (4), 607–662.

Pronk, M., de Kreuk, M.K., de Bruin, B., Kamminga, P., Kleerebezem, R., van Loosdrecht, M.C.M., 2015. Full scale performance of the aerobic granular sludge process for sewage treatment. Water Res. 84, 207–217. https://doi.org/10.1016/j.watres.2015.07.011.

Pronk, M., van Dijk, E.H., van Loosdrecht, M.C.M., 2020. Aerobic Granular Sludge. *Biological Wastewater Treatment; Principles, Modelling and Design (p. 866)*. IWA Publishing London, UK.

Pronk, M., Giesen, A., Thompson, A., Robertson, S., Van Loosdrecht, M., 2017. Aerobic granular biomass technology: advancements in design, applications and further developments. Water Pract. Technol. 12, 987–996. https://doi.org/10.2166/wpt.2017.101.

Rosenzweig, R., Shavit, U., Furman, A., 2012. Water retention curves of biofilm-affected soils using xanthan as an analogue. Soil Sci. Soc. Am. J. 76, 61–69.

ROYAL HASKONINGDHV, 2020. Kaumera Nereda® Gum: A New Innovation in Resource Recovery [WWW Document]. URL. https://www.royalhaskoningdhv.com/en-gb/specials/kaumera. accessed 5.30.21.

Schambeck, C.M., Girbal-Neuhauser, E., Böni, L., Fischer, P., Bessière, Y., Paul, E., da Costa, R.H.R., Derlon, N., 2020. Chemical and physical properties of alginate-like exopolymers of aerobic granules and flocs produced from different wastewaters. Bioresour. Technol. 312, 123632. https://doi.org/10.1016/j.biortech.2020.123632.

Seviour, T., Derlon, N., Dueholm, M.S., Flemming, H.C., Girbal-Neuhauser, E., Horn, H., Kjelleberg, S., van Loosdrecht, M.C.M., Lotti, T., Malpei, F., Nerenberg, R., Neu, T.R., Paul, E., Yu, H., Lin, Y., et al., 2019. Extracellular polymeric substances of biofilms: suffering from an identity crisis. Water Res. 151, 1–7. https://doi.org/10.1016/j.watres.2018.11.020.

Seviour, T., Lambert, L.K., Pijuan, M., Yuan, Z., 2010. Structural determination of a key exopolysaccharide in mixed culture aerobic sludge granules using NMR spectroscopy. Environ. Sci. Technol. 44, 8964–8970. https://doi.org/10.1021/es102658s.

Seviour, T., Pijuan, M., Nicholson, T., Keller, J., Yuan, Z., 2009a. Gel-forming exopolysaccharides explain basic differences between structures of aerobic sludge granules and floccular sludges. Water Res. 43, 4469–4478. https://doi.org/10.1016/j.watres.2009.07.018.

Seviour, T., Pijuan, M., Nicholson, T., Keller, J., Yuan, Z., 2009b. Understanding the properties of aerobic sludge granules as hydrogels. Biotechnol. Bioeng. 102, 1483–1493. https://doi.org/10.1002/bit.22164.

Seviour, T., Yuan, Z., van Loosdrecht, M.C.M., Lin, Y., 2012. Aerobic sludge granulation: a tale of two polysaccharides? Water Res. 46 (15), 4803–4813. https://doi.org/10.1016/j.watres.2012.06.018.

Sikorski, P., Mo, F., Skjåk-Bræk, G., Stokke, B.T., 2007. Evidence for egg-box-compatible interactions in calcium - alginate gels from fiber x-ray diffraction. Biomacromolecules 8 (7), 2098–2103. https://doi.org/10.1021/bm0701503.

Smith, P.K., Krohn, R.I., Hermanson, G.T., Mallia, A.K., Gartner, F.H., Provenzano, M.D., Fujimoto, E.K., Goeke, N.M., Olson, B.J., Klenk, D.C., 1985. Measurement of protein using bicinchoninic acid. Anal. Biochem. 150 (1), 76–85. https://doi.org/10.1016/0003-2697(85)90442-7.

Tay, J.H., Liu, Q.S., Liu, Y., 2001. The role of cellular polysaccharides in the formation and stability of aerobic granules. Lett. Appl. Microbiol. 33 (3), 222–226. https://doi.org/10.1046/j.1472-765X.2001.00986.x.

van Der Roest, H., van Loosdrecht, M.C.M., Langkamp, E.J., Uijterlinde, C., 2015. Recovery and reuse of alginate from granular Nereda sludge. Water 21 17, 48.

van Leeuwen, K., de Vries, E., Koop, S., Roest, K., et al., 2018. The energy & raw materials factory: role and potential contribution to the circular economy of The Netherlands. Environ. Man 61, 786–795. https://doi.org/10.1007/s00267-018-0995-8.

Wang, S., Huang, X., Liu, L., Yan, P., Chen, Y., Fang, F., Guo, J., 2021. Insight into the role of exopolysaccharide in determining the structural stability of aerobic granular sludge. J. Environ. Manag. 298, 113521. https://doi.org/10.1016/j.jenvman.2021.113521.

Wei, Y., Van Houten, R.T., Borger, A.R., Eikelboom, D.H., Fan, Y., 2003. Minimization of excess sludge production for biological wastewater treatment. Water Res. 37 (18), 4453–4467. https://doi.org/10.1016/S0043-1354(03)00441-X.

Xu, J., Pang, H., He, J., Wang, M., Nan, J., Li, L., 2019. Enhanced aerobic sludge granulation by applying carbon fibers as nucleating skeletons. Chem. Eng. J. 373, 946–954. https://doi.org/10.1016/j.cej.2019.05.126.

Zhu, L., Lv, M., Le, Dai, X., Yu, Y.W., Qi, H.Y., Xu, X.Y., 2012. Role and significance of extracellular polymeric substances on the property of aerobic granule. Bioresour. Technol. 107, 46–54. https://doi.org/10.1016/j.biortech.2011.12.008.